Physical Mechanism of the Two-Dimensional Inverse Energy Cascade

Shiyi Chen,[1,2,3,5] Robert E. Ecke,[3,4] Gregory L. Eyink,[1,2,3] Michael Rivera,[4] Minping Wan,[1] and Zuoli Xiao[1]

[1]*Department of Mechanical Engineering, The Johns Hopkins University, Baltimore, Maryland 21218, USA*
[2]*Applied Mathematics & Statistics, The Johns Hopkins University, Baltimore, Maryland 21218, USA*
[3]*Center for Nonlinear Studies and Theoretical Division, Los Alamos National Laboratory, Los Alamos, New Mexico 87545, USA*
[4]*Materials Science & Technology Division, Los Alamos National Laboratory, Los Alamos, New Mexico 87545, USA*
[5]*College of Engineering, 60 Yan-Nan Yuan, Peking University, P.O. Box 100871, Beijing, China*

(Received 6 October 2005; published 28 February 2006)

We study the physical mechanisms of the two-dimensional inverse energy cascade using theory, numerics, and experiment. Kraichnan's prediction of a $-5/3$ spectrum with constant, negative energy flux is verified in our simulations of 2D Navier-Stokes equations. We observe a similar but shorter range of inverse cascade in laboratory experiments. Our theory predicts, and the data confirm, that inverse cascade results mainly from turbulent stress proportional to small-scale strain rotated by 45°. This ''skew-Newtonian'' stress is explained by the elongation and thinning of small-scale vortices by large-scale strain which weakens their velocity and transfers their energy upscale.

DOI: 10.1103/PhysRevLett.96.084502 PACS numbers: 47.27.Ak, 47.27.Gs, 47.27.Jv, 92.60.hk

Inverse energy cascade is a spectacular phenomenon in two-dimensional (2D) turbulent fluids [1–7] and in quasi-2D flows such as planetary-scale atmospheres [8,9]. This energy transfer from small scales sustains large-scale circulations in the flow [10–13] and results in a steady-state inertial range with power-law scaling, as first predicted by Kraichnan nearly 40 years ago [1]. The mechanism of the 2D inverse cascade, however, is controversial. One view is that inverse cascade results from vortex merger, the process whereby smaller vortices combine to form larger ones [1,14,15]. Although mergers play a key role in decaying 2D turbulence [14], there is no sustained inverse cascade in that case. A more recent suggestion, based on qualitative observations from numerics [4] and experiment [6], is that merger does not play a large role in the steady state and inverse cascade is attributed instead to a clustering of like-sign vortices. Another phenomenological explanation of inverse energy cascade is by a Newtonian stress with negative eddy viscosity [16]. Kraichnan [17] gave an intuitive explanation of negative viscosity as a result of ''thinning'' of small-scale vortices by strain at very much larger scales. This heuristic idea has also gained support among geophysicists [18], but no *quantitative* connection between a particular process and local inverse energy cascade has yet been found.

Through a synthesis of numerical simulation, laboratory experiment, and analytical theory, we have developed a quantitative description that accounts for all aspects of inverse cascade. We find strong support for Kraichnan's thinning picture as the mechanism of local cascade. We show, however, that thinning produces not an eddy viscosity as its 1st-order effect but instead a novel stress proportional to ''skew strain,'' or strain rotated by 45°. An important consequence is that the 2D inverse cascade is only weakly local in scale. The thinning mechanism is found to be common to our numerical and experimental systems, which represent very different physical regimes.

We numerically computed the forced Navier-Stokes solution for the velocity $\mathbf{u}$ and vorticity ω in wave number space in a square domain with side $L = 2\pi$ and periodic boundary conditions. A stirring force was applied at wave number $k = 500$ to give a constant energy input rate. Hyperviscous dissipation proportional to $(-\Delta)^{p_u}\omega$ was employed as damping at high k in the equation for ω, with $p_u = 1$ (ordinary viscosity) and $p_u = 8$ (to extend the inertial range). Hypoviscosity $(-\Delta)^{-p_i}\omega$ with $p_i = 2$ was used to damp box-size vortices at small k. The equation was solved using a fully dealiased, parallel pseudo-spectral code with 2nd-order Adam-Bashforth time stepping. The space resolution was 2048^2. A statistically stationary state was achieved after more than 100 large-eddy turnover times. We obtain about two decades of inertial scaling for the hyperviscosity simulations and about one decade using normal viscosity. Since the results of the two simulations are entirely consistent, we report only on the former here.

The laboratory experiment consisted of an electromagnetically forced layer [6] of salt water 3 mm thick and 18 cm × 18 cm in lateral extent. A heavier 3 mm thick buffer layer of Fluorinert, which is immiscible in water, lubricated the upper layer, increasing the stratification and significantly lengthening the run time compared to previous experiments [6]. The effective damping at large scales is linear drag, while dissipation at small scales arises from normal fluid viscosity. The experiments had about half a decade of inverse energy cascade. Velocity fields were obtained using particle tracking velocimetry, resolving velocities on a 100 × 100 spatial grid. For details of the experiment, see [19]. Given the differences between the numerical and experimental systems, any mechanisms of

inverse cascade that are common to both should be robust and universal.

Shown in Figs. 1(a) and 1(b) are energy spectra, $E(k) = \pi k\langle|\hat{\mathbf{u}}(\mathbf{k})|^2\rangle$ for the simulation and experiment. Kraichnan predicted an energy spectrum proportional to $k^{-5/3}$ in 2D [1], just as in the 3D theory of Kolmogorov [20], but with flux of energy towards larger spatial scales. Our results in Fig. 1 are consistent with Kraichnan's prediction although the experiments do not have a large enough range to adequately test for power-law scaling.

In this Letter, we focus on the energy flux across a length scale l in the inertial range, using a filtering approach [21] to resolve fields both in space and in scale. For any smooth, rapidly-decaying filter kernel $G_l(\mathbf{r}) = l^{-2}G(\mathbf{r}/l)$, the convolution $\bar{\mathbf{u}}(\mathbf{x}) = (G_l * \mathbf{u})(\mathbf{x})$ is a low-pass filtered field containing the information from $\mathbf{u}(\mathbf{x})$ only at length scales $>l$. Unlike Fourier or spectral methods, however, this filtering technique preserves information about spatial structures in the flow. Furthermore, the filtered velocity $\bar{\mathbf{u}}(\mathbf{x})$ is easily calculated from the data for the full velocity $\mathbf{u}(\mathbf{x})$ obtained both by direct numerical simulation (DNS) and by experiment. The same approach was used by us earlier to investigate the mechanisms of the 2D direct enstrophy cascade [22].

In this framework, the balance equation for the large-scale kinetic energy density $\bar{e} \equiv (1/2)|\bar{\mathbf{u}}|^2$ is [21]

$$\partial_t \bar{e} + \boldsymbol{\nabla} \cdot \bar{\mathbf{J}} = -\Pi - D, \tag{1}$$

where D is the large-scale damping, $\bar{\mathbf{J}}$ is spatial energy transport, and

$$\Pi = -\bar{\mathbf{S}}{:}\boldsymbol{\tau} = -\bar{S}_{ij}\tau_{ij} \tag{2}$$

is the energy flux to scales $<l$ at each space point. Here $\boldsymbol{\tau} = \overline{\mathbf{u}\mathbf{u}} - \bar{\mathbf{u}}\,\bar{\mathbf{u}}$ is the stress tensor induced by eddies at scales $<l$. The scalar product (2) of the strain tensor $\bar{\mathbf{S}}$ from scales $>l$ and the stress tensor $\boldsymbol{\tau}$ from scales $<l$ gives the rate of work done by the large scales on the small scales. It is positive (forward cascade) when the small-scale stress resists the large-scale strain and positive work is done, and it is negative (inverse cascade) when the stress reinforces the strain and negative work is done. The spatial distributions of Π are shown for our two systems in Figs. 2(a) and 2(b), using a Gaussian filter kernel G to analyze the data [21]. Regions of both forward and inverse cascade are observed but the cascade is backward on average, as shown by the negative mean fluxes plotted as insets in Figs. 1(a) and 1(b). In the numerical simulation [Fig. 1(a)], there is an inertial range of more than a decade where the mean flux is constant, larger than in any previously published simulation [2–5]. There is no clean inertial range in the experiment, but there is a distinct interval of negative mean flux. A major goal of our Letter is to identify the physical processes leading to the regions of positive and negative flux in Figs. 2(a) and 2(b).

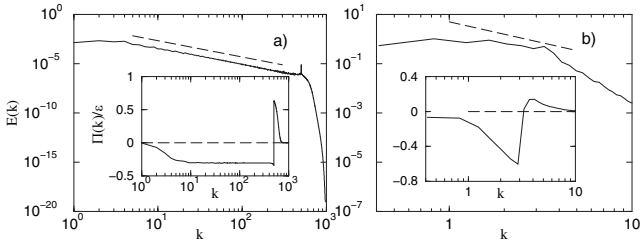

FIG. 1. Energy spectra $E(k)$ vs k at steady state: (a) DNS and (b) experiment (cgs units) with dotted line of slope $-5/3$. Insets: spectral energy flux $\Pi(k)/\epsilon$ vs k for (a) DNS and (b) experiment. ϵ is the net energy dissipation at all scales.

To gain insight into the physical mechanisms we have developed a novel analytical approach [23]: a multiscale gradient (MSG) expansion of the turbulent stress tensor $\boldsymbol{\tau}$. Let $\mathbf{u}^{(n)}$ be the velocity field filtered just as above, but at a small length scale $l_n = 2^{-n}l < l$. We then expand the stress into a convergent series of quadratic products of mth order gradients $\boldsymbol{\nabla}^m\mathbf{u}^{(n)}$ of the velocity at scale l_n. At 1st order in gradients, $m = 1$, we obtain

$$\boldsymbol{\tau}^{(n)}_{\mathrm{MSG}} = C^{(n)} l_n^2 \omega^{(n)} \tilde{\mathbf{S}}^{(n)} \tag{3}$$

for the contribution to stress from length scale l_n [23]. Here $C^{(n)}$ is a positive constant that depends on the filter, $\omega^{(n)}$ is the vorticity at scale l_n and $\tilde{\mathbf{S}}^{(n)}$ is the strain matrix $\mathbf{S}^{(n)}$ at scale l_n rotated counterclockwise by 45°. We refer to $\tilde{\mathbf{S}}^{(n)}$ as skew strain since it is orthogonal to the strain $\mathbf{S}^{(n)}$ in the matrix scalar product. Although $C^{(n)} l_n^2 \omega^{(n)}$ has dimensions

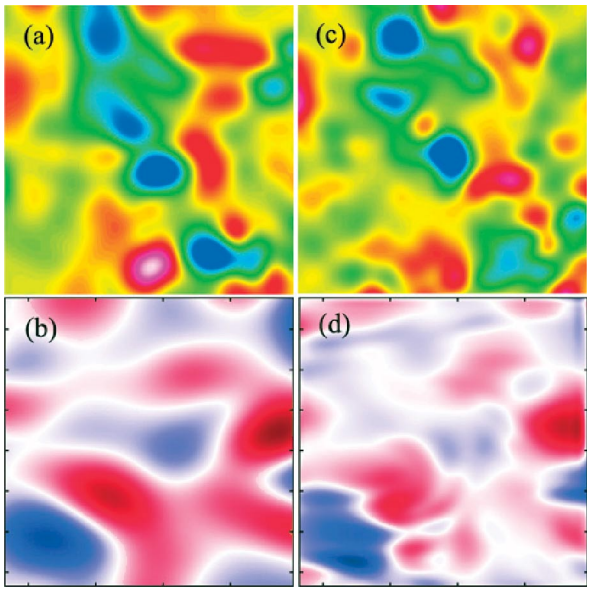

FIG. 2 (color). Instantaneous snapshot of filtered energy flux. Exact flux Π from (a) DNS, $l = \pi/15$ and (b) experiment, $l = 3$ cm and the theoretical MSG flux Π_{MSG} (defined below) at the same length-scales l for (c) DNS and (d) experiment. Negative flux is indicated by blue-green (DNS) and blue (experiment), while positive flux is indicated by red-orange (DNS) and red (experiment).

of viscosity, the stress $\boldsymbol{\tau}^{(n)}_{\mathrm{MSG}}$ is not at all Newtonian, i.e., proportional to strain. Thus, it is quite distinct from the negative eddy viscosity that has often been postulated [16,17].

Before we make a quantitative comparison of this theory with data from our simulation and experiment, we present a simple physical picture of 2D inverse cascade that explains the novel stress law (3). A small-scale vortex embedded in a large-scale strain field will be elongated along its stretching direction and thinned along its compressing direction, creating a long, narrow shear layer [24], as illustrated in Fig. 3. Kelvin's theorem, or conservation of circulation, then requires that the velocity around the vortex be weakened, reducing its energy. Simultaneously, this velocity will be rectified to lie mostly parallel to the stretching axis, producing a net positive or tensile stress along that direction. Because this stress acts to reinforce the large-scale strain, the energy lost by the small-scale vortex is transferred to the large scales. The small-scale strain in the narrow shear layer is oriented at $\pm 45°$ with respect to the large-scale strain, $\pm$ depending upon the sign of the small-scale vorticity. Thus, the stress is proportional to $\omega^{(n)}\tilde{\mathbf{S}}^{(n)}$, consistent with our analytical result. This mechanism is similar to the vortex thinning proposed by Kraichnan [17] to explain the origin of negative eddy viscosity.

We now examine the quantitative predictions of our analytical theory. We have used the data from our simulations and experiments to evaluate the flux Π_{MSG} predicted by the MSG expansion, including all subscale contributions for $n \geq 0$ and up to 2nd order in gradients ($m = 1, 2$). Two new stress contributions arise at that order, which can be shown theoretically to lead also to inverse cascade as a consequence of vortex thinning [25]. We find from analysis of the data that the space average of Π_{MSG} overpredicts the mean of the true flux Π by just 10%. Of this result about 70% comes from the 1st-order skew-strain term. The spatial correlation of $\Pi_{\mathrm{MSG}}(\mathbf{x})$ pointwise with the true $\Pi(\mathbf{x})$ is 0.89 after $\Pi_{\mathrm{MSG}}(\mathbf{x})$ is refiltered to remove fine scale features introduced by the subgrid contributions with $n > 1$. This refiltered field is plotted in Figs. 2(c) and 2(d), for DNS and experiment, respectively. The theoretical result, Π_{MSG}, very closely resembles the true flux Π pointwise in space: inverse cascade occurs in the regions of vortex thinning, as predicted. Gathering statistics from many flow realizations yields the probability distribution function (PDF) of the flux shown in Figs. 4(a) and 4(b) for DNS and experiment, respectively. The PDFs of the MSG model flux capture well the negative skewness in the PDFs of the exact flux, with just slightly suppressed tails due to the refiltering. The agreement between the numerical and experimental systems is remarkable.

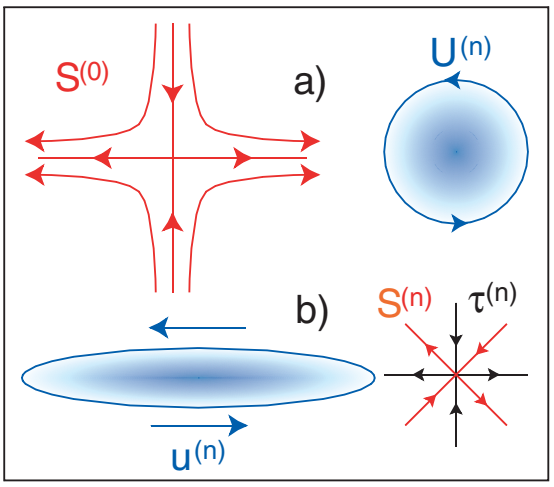

FIG. 3 (color). Vortex-thinning mechanism: (a) small-scale circular vortex (blue) in a large- scale strain-field $\mathbf{S}^{(0)}$ (red); (b) small-scale vortex drawn out into a narrow shear layer with weakened velocity $u^{(n)} < U^{(n)}$. The axes of the small-scale stress tensor $\boldsymbol{\tau}^{(n)}$ (black) are aligned with those of the large-scale strain $\mathbf{S}^{(0)}$ whereas the small-scale strain $\mathbf{S}^{(n)}$ axes are rotated $\pm 45°$ with respect to $\mathbf{S}^{(0)}$.

Another prediction of the theory is the degree of scale locality of the cascade, i.e., the contribution to the flux from different subgrid scales n. This is quantified by the flux fraction from each length-scale l_n, defined as the average of the flux $\Pi^{(n)} = -\bar{\mathbf{S}}{:}\boldsymbol{\tau}^{(n)}$ due to stress from that scale, normalized by the total mean flux. (The stress $\boldsymbol{\tau}^{(n)}$ from length scale l_n can be calculated as the stress due to $\mathbf{u}^{(n)}$ minus the stress due to $\mathbf{u}^{(n-1)}$, for $n \geq 1$.) It is a direct consequence of the thinning mechanism that very little of the cascade arises from stress at the same scale ($n = 0$) as the strain $\bar{\mathbf{S}}$. To first order in gradients, the strongly scale-local ($n = 0$) contribution to flux is exactly zero, because of the orthogonality of strain and skew strain at the same scale. The vanishing of the $n = 0$ contribution pointwise in space can be attributed also to the absence of vortex stretching in 2D [23], extending a result of Kraichnan for spectral flux [26].

In Fig. 5, the flux fractions are plotted from DNS, both for true flux and the MSG model up to 2nd order. Note that

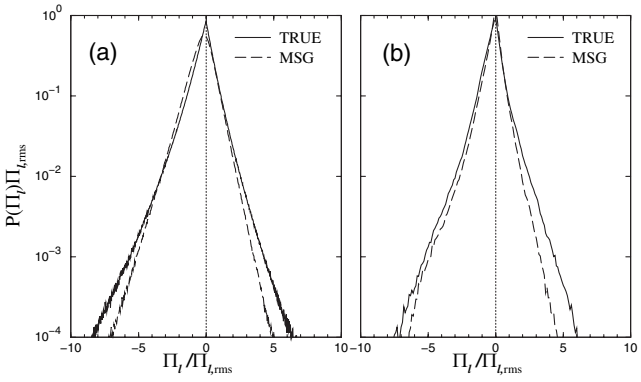

FIG. 4. Normalized PDFs of true energy flux Π and the model flux Π_{MSG}, using the same filter scales l as in Fig. 2, for (a) DNS and (b) experiment.

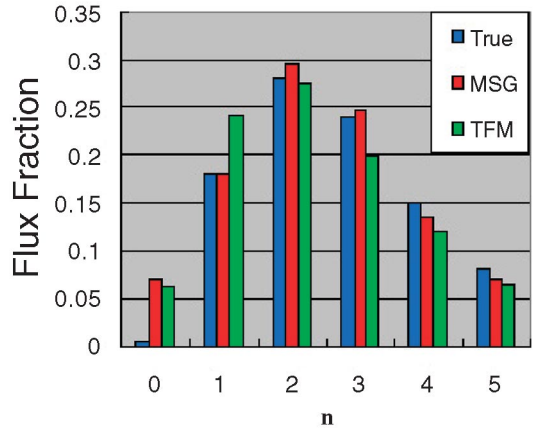

FIG. 5 (color). Flux fraction $\langle \Pi^{(n)} \rangle / \langle \Pi \rangle$ from each scale l_n. Shown are the exact and MSG results from DNS, and, for comparison, the TFM predictions.

the exact flux for $n = 0$ is nearly zero and the 2nd-order MSG result is also very small. The exact result confirms not only the weak locality of the cascade but also the fact that $\boldsymbol{\tau}^{(0)} \propto \tilde{\mathbf{S}}^{(0)}$ to a good approximation, as predicted by (3). Indeed, the $n = 0$ contribution to flux can vanish *only* if the angle θ between eigenframes of $\mathbf{S}^{(0)}$ and $\boldsymbol{\tau}^{(0)}$ is $\pm 45°$. [Note that the matrix inner-product $\mathbf{S}^{(0)}:\boldsymbol{\tau}^{(0)}$ is proportional to $\cos(2\theta)$.] Fig. 5 shows that the 2nd-order MSG results for flux fraction match the exact results well also for $n > 0$. We see that most of the mean flux results from vorticity 4–8 times smaller than the resolved scales, i.e., from subscale bands $n = 2$–3. This result is consistent with the prediction of Kraichnan's test-field mode (TFM) closure [26] which is also plotted in Fig. 5. The excellent agreement is further evidence for our theoretical interpretation of the inverse energy cascade in terms of vortex thinning.

The results we have presented give new physical understanding of the 2D inverse energy cascade. The mechanism is closely related to that for forward enstrophy cascade in 2D, which results also from vortex thinning, by steepening of inertial-range vorticity gradients [22]. Note that the curl of the skew-Newtonian stress in (3) yields the vorticity transport vector $(\boldsymbol{\nabla} \mathbf{u}^{(n)}) \boldsymbol{\nabla} \omega^{(n)}$ which, for $n = 0$, was verified in [22] to account for nearly all of the enstrophy flux in the forward cascade range. Although related, inverse energy cascade is a more subtle phenomenon than forward enstrophy cascade. Enstrophy flux across a length l in the forward cascade range results from thinning of 2D vortices of size l by strains from length scales up to the injection scale $L \gg l$ (infrared-nonlocality). On the other hand, energy flux across a length l in the inverse cascade range is due to thinning of subscale vortices 4–8 times smaller than l by strain at length scale l (weak ultraviolet locality). Although inverse energy cascade is much more scale local than direct enstrophy cascade, it is more difficult to model because of the essential contribution of subscale vortices.

The thinning picture and our analytical expansion make other detailed predictions, whose verification will be presented elsewhere. An important remaining issue for fundamental theory is to clarify the dynamical origins of the correlations we have identified as crucial to inverse cascade. The multiscale gradient expansion that was presented here should have important applications to modeling of turbulence in diverse geophysical and astrophysical settings.

[1] R. H. Kraichnan, Phys. Fluids **10**, 1417 (1967).
[2] M. E. Maltrud and G. K. Vallis, J. Fluid Mech. **228**, 321 (1991).
[3] L. Smith and V. Yakhot, Phys. Rev. Lett. **71**, 352 (1993).
[4] G. Boffetta *et al.*, Phys. Rev. E **61**, R29 (2000).
[5] K. S. Smith *et al.*, J. Fluid Mech. **469**, 13 (2002).
[6] J. Paret and P. Tabeling, Phys. Rev. Lett. **79**, 4162 (1997); Phys. Fluids **10**, 3126 (1998).
[7] M. A. Rutgers, Phys. Rev. Lett. **81**, 2244 (1998).
[8] K. S. Gage, J. Atmos. Sci. **36**, 1950 (1979); K. S. Gage and G. D. Nastrom, J. Atmos. Sci. **43**, 729 (1986).
[9] D. K. Lilly, J. Atmos. Sci. **46**, 2026 (1989).
[10] J. Sommeria *et al.*, Nature (London) **331**, 689 (1988).
[11] P. S. Marcus, Nature (London) **331**, 693 (1988).
[12] M. A. Abramowicz *et al.*, Nature (London) **356**, 41 (1992).
[13] M. S. Lozier, Science **277**, 361 (1997).
[14] J. C. McWilliams, J. Fluid Mech. **219**, 361 (1990); W. H. Matthaeus *et al.*, Phys. Rev. Lett. **66**, 2731 (1991); D. G. Dritschel, Phys. Fluids A **5**, 984 (1993).
[15] A. H. Nielsen *et al.*, Phys. Fluids **8**, 2263 (1996); R. Irion, Science **284**, 1609 (1999); X. Carton *et al.*, J. Turbulence **3**, 45 (2002).
[16] V. P. Starr, *Physics of Negative Viscosity Phenomena* (McGraw-Hill, New York, 1968).
[17] R. H. Kraichnan, J. Atmos. Sci. **33**, 1521 (1976).
[18] P. B. Rhines, Annu. Rev. Fluid Mech. **11**, 401 (1979); R. Salmon, *Lectures on Geophysical Fluid Dynamics* (Oxford University, Oxford, 1998).
[19] M. Rivera and R. Ecke, cond-mat/0512214.
[20] A. N. Kolmogorov, Dokl. Akad. Nauk SSSR **30**, 301 (1941).
[21] M. Germano, J. Fluid Mech. **238**, 325 (1992); G. L. Eyink, J. Stat. Phys. **78**, 335 (1995); C. Meneveau and J. Katz, Annu. Rev. Fluid Mech. **32**, 1 (2000).
[22] M. K. Rivera *et al.*, Phys. Rev. Lett. **90**, 104502 (2003); S. Chen *et al.*, Phys. Rev. Lett. **91**, 214501 (2003).
[23] G. L. Eyink, J. Fluid Mech. **549**, 191 (2006).
[24] S. Kida, J. Phys. Soc. Jpn. **50**, 3517 (1981).
[25] The new terms in the MSG expansion at 2nd order are a Newtonian stress $-\nu_T \mathbf{S}^{(n)}$ with eddy viscosity ν_T associated to differential strain rotation and a tensile stress directed along isovorticity lines, from vorticity-gradient stretching. See [23] for a detailed discussion.
[26] R. H. Kraichnan, J. Fluid Mech. **47**, 525 (1971).